Polymer Testing 28 (2009) 277–287

Contents lists available at ScienceDirect

Polymer Testing

journal homepage: www.elsevier.com/locate/polytest

Test Method

# Study of the dispersion of nanoclays in a LDPE matrix using microscopy and in-process ultrasonic monitoring

M.P. Villanueva [a,*], L. Cabedo [a], E. Giménez [a], J.M. Lagarón [b], P.D. Coates [c], A.L. Kelly [c]

[a] Area of Materials, Department of Industrial Systems Engineering and Design, University Jaume I, Avda. Vicent Sos Baynat s/n, 12071 Castellón, Spain
[b] Novel Materials and Nanotechnology, Institute of Agrochemistry and Food Technology (IATA-CSIC), Apdo. Correos 73, Burjassot 46100, Valencia, Spain
[c] IRC in Polymer Engineering, School of Engineering, Design and Technology, University of Bradford, Bradford BD7 1DP, United Kingdom

ARTICLE INFO

*Article history:*
Received 5 November 2008
Accepted 22 December 2008

*Keywords:*
Polyethylene
Nanocomposites
Organoclay
Kaolinite
Montmorillonite
Dispersion
Ultrasound attenuation

ABSTRACT

LDPE/montmorillonite and LDPE/kaolinite compounds were prepared by twin-screw extrusion using two screw profiles. The microstructure of the samples was determined by a combination of techniques: wide angle X-ray scattering (WAXS), optical microscopy (OM), scanning electron microscopy (SEM), transmission electron microscopy (TEM) and small amplitude rheometry. This work presents also a new technique as a macroscopic measurement of the morphology of bulk filled polymers: in-line monitoring of low energy ultrasound waves during melt extrusion. Transit time, signal loss and peak height of ultrasound waves transmitted through the melt polymer were measured for all the samples. These parameters appeared to provide significant information of dispersion levels or aggregate size, and maintained a good correlation with the microscopic studies and the rheological data.



## 1. Introduction

Polymer-layered silicate nanocomposites are of especial importance because of the significant improvement in mechanical, thermal and barrier properties that can be achieved with the incorporation of a low nanoclay loading [1–3]. Particularly, polyethylene is one of the most commercially important polyolefins with a wide field of applications, and the improvement of its physical properties has been the focus of interest for many researchers [4–6].

There are different methods to prepare nanocomposites, however melt mixing appears to be the most used and the most important from an industrial point of view. Regarding this, it can be said that twin-screw extrusion has emerged as the most effective way to prepare polymer-layered silicate nanocomposites by melt blending. It has been reported that the degree of delamination and dispersion is affected by the type of extruder (single or twin-screw extruder, co-rotating or counter-rotating, intermeshing or non-intermeshing) and its screw design [7]. Screw design is a very important factor to take into account in polymer processing as it affects extruder throughput, rate of melting, mixing, melt temperature, process efficiency and total residence time of the material in the extruder [8,9]. Extrusion process parameters such as screw speed, temperature and feed rate influence also the dispersion of the layered clays [10].

Generally, the methods most commonly used to study the morphology of polymer–clay nanocomposites have been wide angle X-ray scattering (WAXS), scanning electron microscopy (SEM) and transmission electron microscopy (TEM). However, in recent years these techniques have been combined with rheological measurements [11]. Microscopy and rheological tests are off-line measurements and supply information on a small portion of the material. Nevertheless, in-process measurements have the advantage of measuring bulk properties giving information related to melt properties in real time [12].

* Corresponding author. Tel.: +34 964728212; fax: +34 964728170.
*E-mail address:* mvillanu@esid.uji.es (M.P. Villanueva).

0142-9418/$ – see front matter © 2008 Elsevier Ltd. All rights reserved.
doi:10.1016/j.polymertesting.2008.12.009

Low energy ultrasound waves have been used to observe the behaviour and to measure properties of polymers during processing. Ultrasonic transducers connected to the extruder die or to the barrel of the extruder generate pulses which transmit through the melt polymer. Parameters such as transit time (or sound velocity), reflected–transmitted wave height and signal attenuation provide useful information on polymer properties.

In-process ultrasound measurements have been carried out previously during extrusion of polymer blends for measuring the blend ratio [13]. The same technique has been available commercially for some years for polymer product assessments such as wall thickness distribution in extruded pipe [14]. Erwin and Dohner [15] used ultrasound to measure the dispersion of solid additives in polyethylene. Verdier [16] measured the velocities of propagation and attenuation of ultrasonic waves during flow through a capillary rheometer to deduce the concentration and average size of inclusions in polyamide 6 and polypropylene blends. Several studies have reported determination of filler concentration in composites (talc, $TiO_2$, mica and glass fibers) [17] and dispersion of fillers such as carbon black by measuring ultrasound waves [18].

In this work, low density polyethylene (LDPE) was melt mixed with two different clays (montmorillonite and kaolinite) in a twin-screw extruder. Two screw configurations with different shear intensity were used. The influence of extruder screw configuration, the addition of compatibilizer and the clay nature were analysed in terms of the state of clay dispersion. This paper reports on the effect of such parameters on nanocomposite structure, which was examined here by OM, SEM, TEM, WAXS and rotational rheometry. In-line ultrasound measurements were monitored during extrusion as an extra tool to analyse qualitatively the level of dispersion in LDPE nanocomposites.

## 2. Experimental

### 2.1. Materials

Polyethylene nanocomposites based on a LDPE (*Alcudia® PE-015*, Repsol YPF) were prepared with two different types of clay: kaolinite and montmorillonite. The montmorillonite used in this study is a proprietary food contact compliant commercial organomodified clay (oMMT, *Nanobiotер® AE21*) supplied as a powder, and the kaolinite (K) was supplied as a masterbatch composed of a low density polyethylene and a processed kaolinite with no organic modification (*Nanobiotер® D240B*). Both materials were kindly supplied by NanoBioMatters, S.L. (Valencia, Spain). No further details of masterbatch preparation or clay modification were disclosed by the manufacturer. A polyethylene grafted with maleic anhydride (*Fusabond® E MB226DE*, 0.9% of grafting level) hereafter referred to as *PEMA*, was supplied by Dupont Iberica, S.L. (Barcelona, Spain) and was used as a compatibilizer in montmorillonite samples. This grade of PEMA is based on a linear low density polyethylene with a density of 0.93 g/cm$^3$, a melt flow index of 1.5 g/10 min (190 °C/2.16 kg) and a melting temperature of 120 °C. The LDPE used is a commercial grade for film blowing and casting with a density of 0.92 g/cm$^3$ and a melt flow index of 1 g/10 min.

### 2.2. Preparation of polyethylene nanocomposites

Polyethylene nanocomposites were prepared by melt compounding using a co-rotating Thermo-Prism Eurolab twin-screw extruder with screw diameter ($D$) of 16 mm and length to diameter ($L/D$) ratio of 40:1. Two separate feeders were used to feed the polymer pellets and the clay powder (in the case of montmorillonite) into zone 1 of the extruder. The masterbatch of LDPE and kaolinite was fed in the form of pellets. The extruder was equipped with a single strand die with a diameter of 4 mm. Extruded material was cooled in a water bath and pelletised. The montmorillonite and the compatibilizer were dried at 80 °C for 24 h in an oven prior to compounding.

Low density polyethylene and its nanocomposites were extruded with a temperature profile between 170 and 190 °C (zone 2–zone 10) in the barrel of the extruder and 190 °C at the die. The extruder feed throat (zone 1) was water cooled. Screw speed was fixed at 200 rpm. Barrel temperatures and screw speed were kept constant (Table 1).

The samples were extruded with two different screw configurations (configuration 'A' and configuration 'B'). Screw configuration A was set up for intensive mixing and high residence time, with a combination of distributive (forward staggered bi-lobal paddles) and dispersive (non-staggered bi-lobal paddles) mixing sections, with two reverse feed screw elements to further increase residence time and back-mixing. Screw configuration B was set up for more conventional, lower residence time compounding operations, with three purely distributive mixing zones. The residence time measured was approximately 3.08 min for LDPE extruded with configuration A (at 309 g/h and 200 rpm) and 1.14 min for configuration B.

The clay content in all the extruded nanocomposites was approximately 7 wt.-%. A small content of compatibilizer (10 wt.-%.) was added in some montmorillonite samples in an attempt to improve the exfoliation in the LDPE/oMMT system. Although higher compatibilizer contents have been reported to give complete exfoliated morphologies [19], here it is proposed to use a lower content due to the fact that the addition of PEMA can deteriorate properties such as mechanical or barrier, in addition to the increment in the final cost of the material.

**Table 1**
Composition and processing conditions of all the extruded samples.

| Sample | Screw configuration | Feed rate (g/h) | T (°C) | Screw speed (rpm) |
|---|---|---|---|---|
| LDPE | A | 309 | 170–190 | 200 |
| LDPE/oMMT | A | 309 | 170–190 | 200 |
| LDPE/oMMT | B | 309 | 170–190 | 200 |
| LDPE/PEMA/oMMT | A | 178 | 170–190 | 200 |
| LDPE/PEMA | A | 178 | 170–190 | 200 |
| LDPE/K | A | 309 | 170–190 | 200 |

### 2.3. Techniques

#### 2.3.1. Structure and morphological characterization

Optical micrographs were obtained by an optical microscope (Leica model DM-RME). Observations were made in transmission mode on nanocomposite films, prepared by melt pressing, of approximately 100 μm in thickness. The micrographs represented here were obtained with a magnification of 100×.

Scanning electron microscopy (SEM) was also used in order to more closely observe the dispersion of clay in the nanocomposites. Cryofractured samples from the extruded fibre were measured using a Leo SEM (model 440i).

The dispersion of clay layers was also observed by transmission electron microscopy (TEM). Nanocomposites samples were inserted in an epoxy resin and were cut at room temperature in sections of around 90 nm in thickness with an ultramicrotome. The equipment used to observe the sections was a Jeol 1011 (100 kV).

Wide angle X-ray scattering experiments (WAXS) were performed using a Bruker AXS D4 Endeavour diffractometer. Radial scans of intensity versus scattering angle ($2\theta$) were recorded at room temperature in the range 2–30° (step size = 0.02° ($2\theta$), scanning rate = 8 s/step) with identical setting of the instrument by using filtered $CuK_\alpha$ radiation ($\lambda = 1.54$ Å), an operating voltage of 40 kV, and a filament current of 30 mA. To calculate the clay $d$-spacing, Bragg's law ($\lambda = 2d \sin\theta$) was applied.

#### 2.3.2. Rheological characterization

Rheological measurements were performed using a rotational rheometer with two parallel plates (Anton Paar MCR301). Storage modulus and complex viscosity were measured over a frequency range of 0.1–100 rad/s at 190 °C using two plates of 25 mm of diameter. The deformation amplitude was 5%.

Melt strength was measured by a Rosand capillary rheometer (RH10), using a die of 20 mm in length, 2 mm in diameter and entry angle of 180°, and a set temperature of 190 °C. The haul-off equipment attached to the rheometer was used to measure the force required to break the fibre of polymer during fibre spinning. The only parameters that are easy to measure are the haul-off speed at which the fibre breaks and the maximum force at which the fibre breaks. The experimental conditions used in the fibre spinning were a piston speed during threading and during the test of 20 mm/min, a haul-off speed during threading of 2 m/min and during the test an accelerating ramp (2–50 m/min in 5 min).

#### 2.3.3. Mechanical properties

Elastic modulus was obtained from the stress-deformation curves registered in the tests carried out on a universal testing machine (Instron 4469) at a crosshead speed of 10 mm/min and room temperature. Tests were made according to ISO 527 using injection moulded tensile bars.

#### 2.3.4. Ultrasonic characterization

Ultrasonic measurements of extruded polyethylene and nanocomposites were made during extrusion by means of an ultrasonic pulser–receiver (Panametrics 5900PR), a sampling digital oscilloscope (LeCroy 9359AM) and an automated data acquisition system. Two flush-mounted ultrasound transducers were diametrically opposed across the die to transmit and receive ultrasound waves through the melt polymer. The frequency of the longitudinal waves generated by the ultrasonic transducers used was 3.5 MHz and transmitted signals were monitored using a high frequency (1 GHz) oscilloscope. These signals were converted into an array of voltage values representing the magnitude of the received sound wave, and time values calculated from the known trigger time and sampling frequency. Real-time analysis of the received signals was carried out at a frequency of 1 Hz using in-house software (University of Bradford). From the voltage–time waveform array, a measurement of the signal transit time was taken as an indication of the velocity of wave propagation through the fixed distance across the extruder die. The height of the first received wave peak and the percentage drop between first and second peaks were measured as an indication of ultrasonic energy and attenuation (signal loss), respectively. These in-process measurements were made across the melt using the instrumentation unique to the Bradford IRC Polymer Engineering Laboratories.

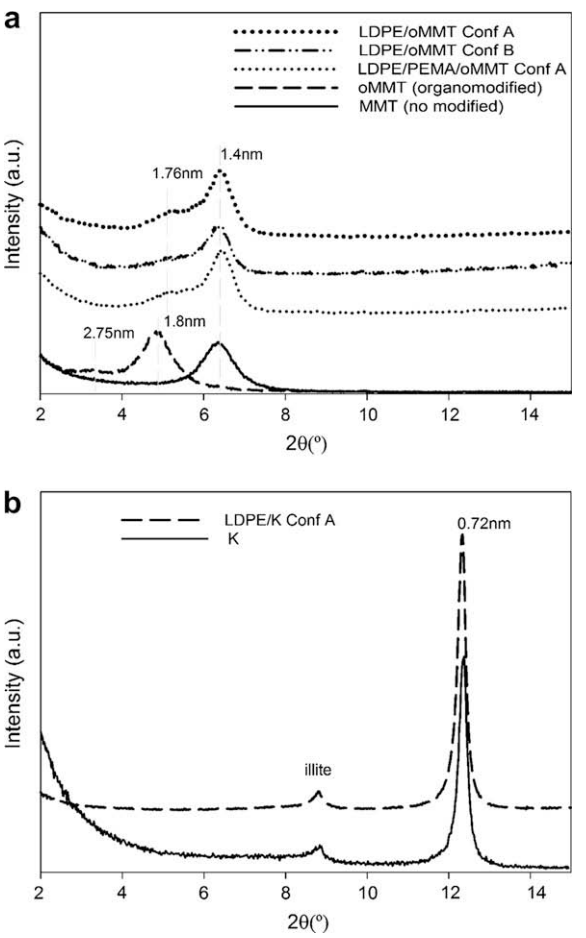


**Fig. 1.** WAXS diffractograms of (a) LDPE/montmorillonite systems; (b) LDPE/kaolinite system.

## 3. Results and discussion

### 3.1. X-ray measurements

Diffractograms obtained for the different polyethylene/montmorillonite systems are reported in Fig. 1a. Patterns of organomodified and natural montmorillonite are also represented.

The diffractogram of the oMMT reveals an intense peak of modified clay corresponding to a basal spacing of 1.8 nm ($2\theta = 4.9^{\circ}$) and a small shoulder to lower angles ($3.2^{\circ}(2\theta)$) belonging to a fraction of clay with basal spacing of 2.75 nm. The position of the (001) peak of the clay was displaced to higher angles in all the compounded samples, probably due to the loss of the surfactant molecules used for the modification of the clay and that are liberated from

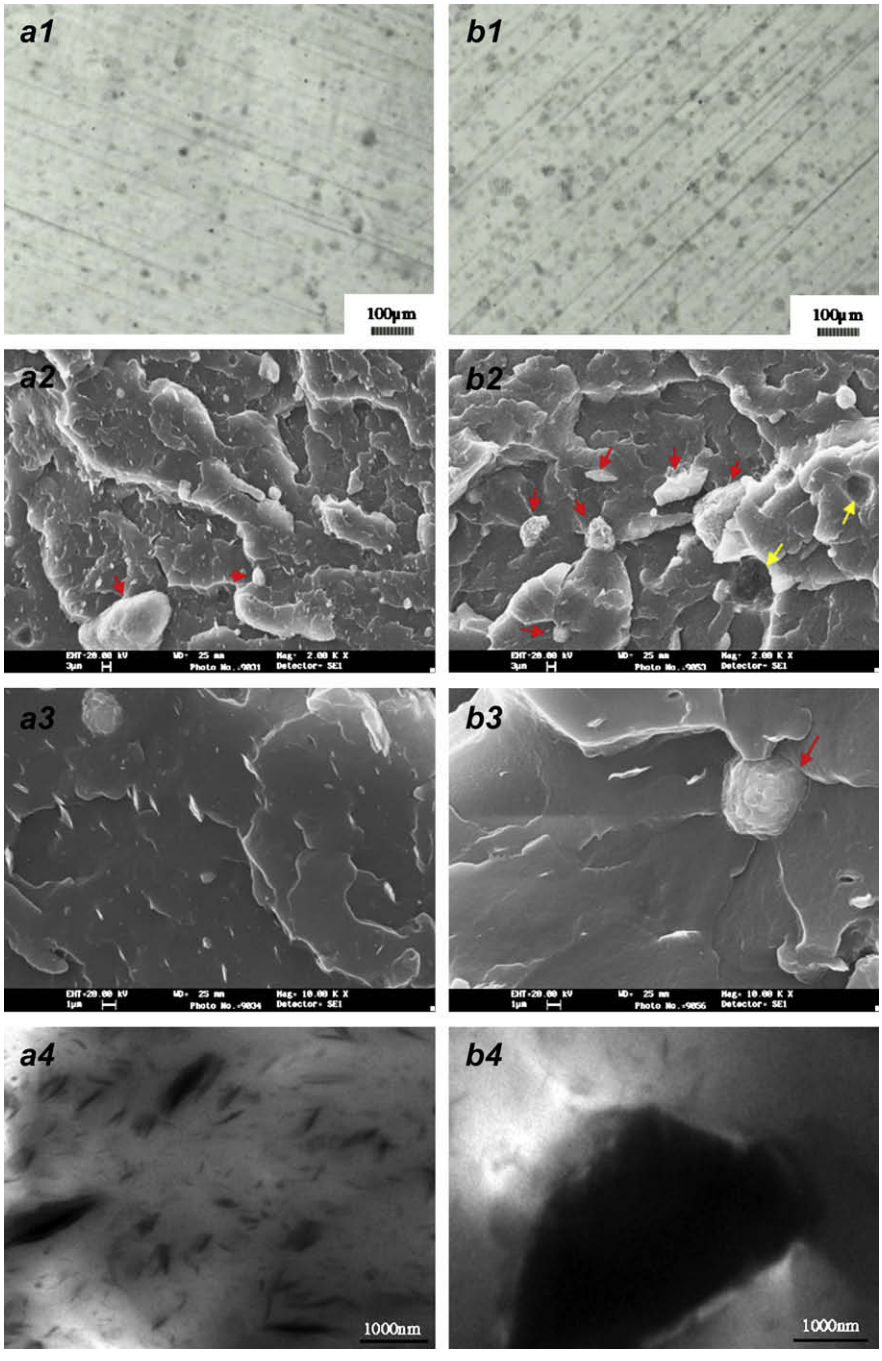


**Fig. 2.** Micrographs of LDPE/oMMT in screw configuration A (series a) and screw configuration B (series b): (*a1*, *b1*) OM; (*a2*, *b2*, *a3*, *b3*) SEM; (*a4*, *b4*) TEM.

the gallery and possibly degraded. The basal peak in the polyethylene compounds is located around 6.4°(2$\theta$) which corresponds to a basal spacing of 1.4 nm. This indicates the low stability of the modification at the processing conditions used (i.e. temperature profile, feed rate, residence time) in the extrusion process and that the layers of clay collapsed during extrusion. The (001) peak position is not varied with the addition of compatibilizer or with different mixing conditions such as screw configuration. However, there is a small shoulder at around 5°(2$\theta$) that could be modified clay (with a basal spacing of 1.76 nm) that is more thermally stable.

Shah et al. [20] attributed the collapse of montmorillonite layers to the degradation of surfactants attached to the clay surface at the processing temperature (from 180 °C depending on the modification). In the samples of the present study, the oMMT received high shear by the different mixing elements of the screws and was exposed at the die to temperatures higher than 190 °C.

Fig. 1b represents the diffraction patterns of the kaolinite used (K) in the received masterbatch and LDPE/K nanocomposite prepared with screw configuration A. The basal zone of the diffractogram shows the diffraction (001) peak of kaolinite located at 12.4°(2$\theta$) which corresponds to a basal spacing of 0.72 nm. This peak was maintained in the nanocomposite, which indicates that there is clay in the aggregated state. The peak that is located at 9°(2$\theta$) refers to the (003) reflection of the illite, which is a minority mineral of the kaolinitic clay used. No clay degradation can be detected in this sample because no organic modifiers were used to treat the kaolinite.

According to WAXS measurements, only aggregated structures can be confirmed in all the samples, but this technique is not sufficient to evaluate the clay dispersion in the different samples. Vergnes et al. [11] reported that X-ray measurements were not sufficient to clearly describe the structures in polypropylene/montmorillonite nanocomposites compounded at different conditions such as mixing time, screw speed mixing temperature and screw profile. In this case, the study was completed with rheological characterization. Recently, in nanocomposites with kaolinite [21], the results obtained by WAXS needed to be completed with SEM and TEM to have clear conclusions about the morphology. Therefore, in this study the morphology was analyzed by microscopy and rheology.

### 3.2. Microscopical observations

#### 3.2.1. Effect of screw configuration

The effect of screw configuration on the morphology of polyethylene nanocomposites was studied in the system with organomodified montmorillonite. Fig. 2 shows the morphology observed by OM, SEM and TEM of the sample LDPE/oMMT extruded at 309 g/h and 200 rpm with screw configuration 'A' (*a1*, *a2*, *a3*, *a4*) and with screw configuration 'B' (*b1*, *b2*, *b3*, *b4*). The comparison between both screw designs shows that the oMMT is better dispersed in the sample extruded with screw configuration 'A'.

Images *a1* and *b1* represent the morphology on the micrometric scale, where it can be seen that the density of microaggregates is higher in the sample processed with screw configuration B. On the nanometric scale, SEM images confirm an aggregated morphology for both screws. The sample processed with configuration A shows a fraction of the clay dispersed below 3 μm (*a2*), while the composite extruded with configuration B shows a high

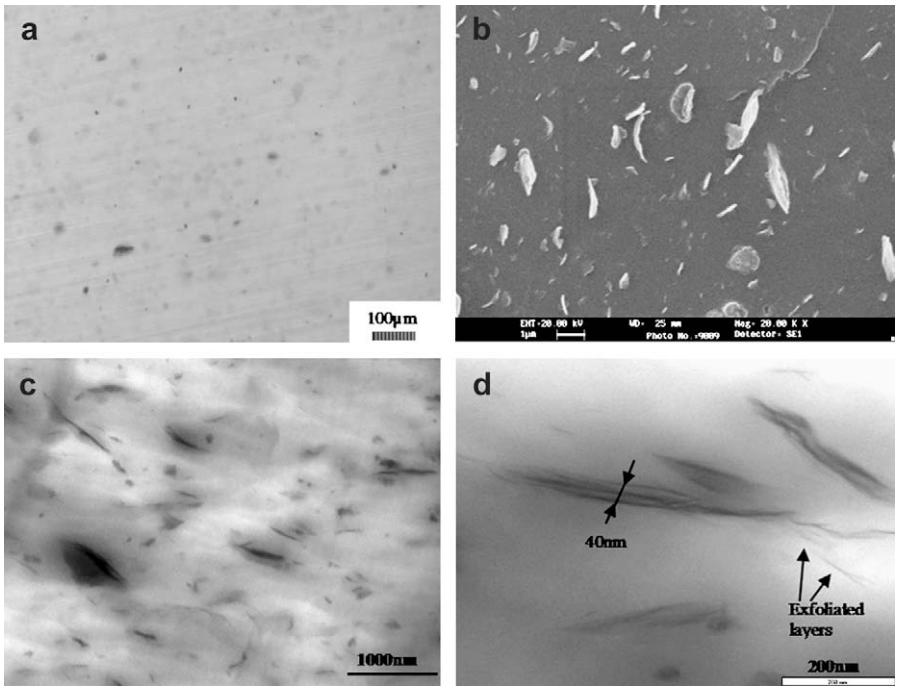


**Fig. 3.** Micrographs of LDPE/PEMA/oMMT nanocomposite: (a) OM; (b) SEM; (c,d) TEM.

concentration of large aggregates between 3 and 10 μm (indicated by arrows), with some holes representing large aggregates with a low adhesion that were peeled off from the surface (*b2*). At a higher magnification (image *a3*) a high density of nanometric aggregates was observed (a few hundreds of nanometers in thickness) in the sample processed with screw configuration A. This confirms that a nanocomposite was obtained. SEM image *b3* exhibits a low density of clay particles; however this is not indicative of good exfoliation because the clay was observed to form large agglomerates (as marked with an arrow) and several large aggregates were also observed at the micrometric scale. Results from samples processed with screw configuration B showed that nanometric particles were not achieved, and this material could be more accurately described as a microcomposite. TEM pictures (*a4* and *a5*) corroborate that no exfoliation was obtained in the LDPE/oMMT samples but small tactoids of a few nanometers in thickness are shown to be dispersed in the sample with screw configuration A. The mixing of the two components by screw configuration B gives the structure typical of a microcomposite or conventional composite.

### 3.2.2. *Effect of addition of compatibilizer*

Many reported research studies on polyolefin nanocomposites have concluded that the incorporation of maleated oligomers (i.e. polyethylene or polypropylene grafted with maleic anhydride) improves the level of exfoliation in the final nanocomposites [5,6]. According to the results obtained in the LDPE/oMMT compounds processed with two screw configurations, it was decided to prepare new samples to study the effect of the addition of a small content of PEMA as a compatibilizer by means of screw configuration A. Fig. 3 shows the morphology of the nanocomposite LDPE/PEMA/oMMT on the micrometric and nanometric scale. Although the optical micrograph (Fig. 3a) shows that there is no complete dispersion of the clay with the incorporation of compatibilizer, the observation by SEM

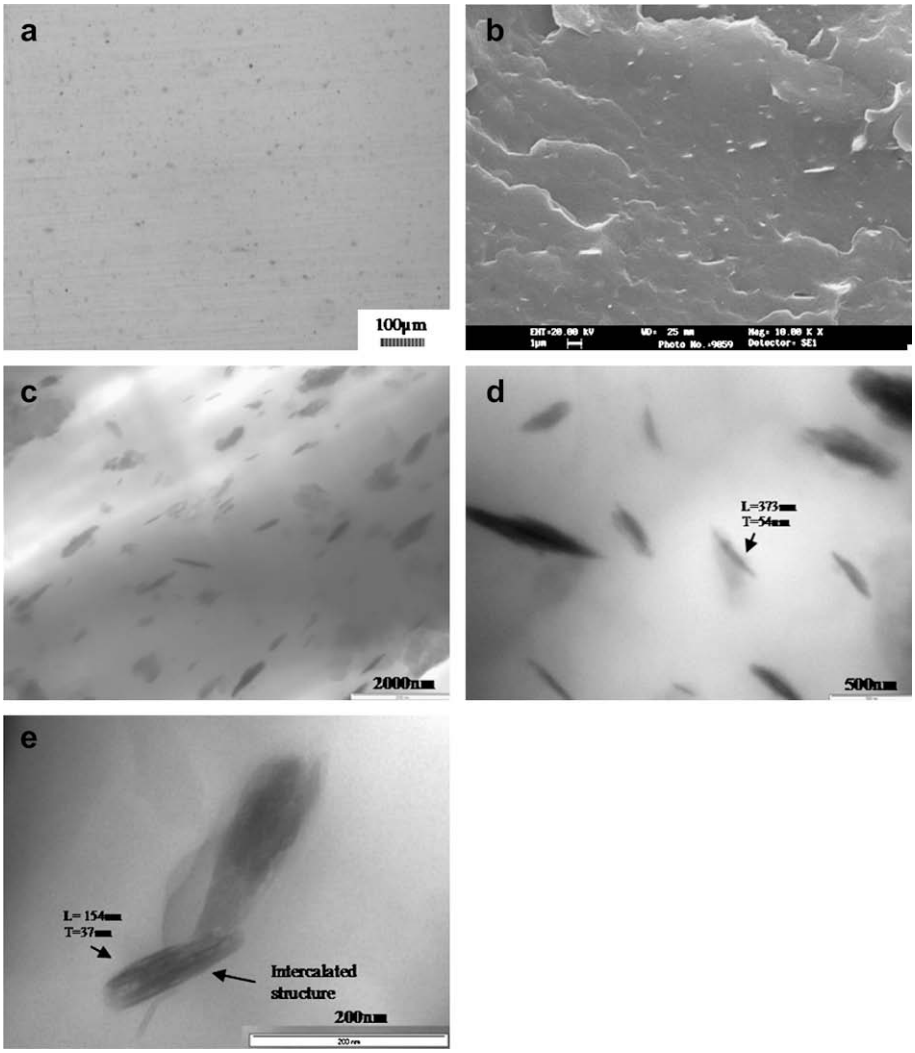


**Fig. 4.** Micrographs of LDPE/K nanocomposite: (a) OM; (b) SEM; (c–e) TEM.

and TEM gives an aggregated–intercalated structure of small tactoids with a thickness of the order of nanometers (Fig. 3b,c scale <1 μm). High magnification TEM micrograph (Fig. 3d) represents an intercalated structure formed by a few tactoids of high aspect ratio (length ~300–400 nm, thickness ~10 nm) and some exfoliated layers around the intercalated tactoids.

### 3.2.3. Effect of clay nature

Much of the reported literature regarding polyolefin/clay nanocomposites has centred on the development of different formulations based on montmorillonitic clays, exploring different processing conditions and different oligomers as compatibilizers. In this paper we present the results of a preliminary study on the dispersion of a different clay (kaolinite) in polyethylene. Although there are some reported studies about the effect of kaolinite in other polymeric matrices [21–24], the influence in polyolefinic matrices is still not reported.

As previously stated, LDPE/K nanocomposite was prepared from a masterbatch containing kaolinite with no organic modification. The morphology of the sample LDPE/K is shown in Fig. 4. Kaolinite was homogeneously dispersed in the polyethylene matrix and the density and the size of microaggregates (Fig. 4a) were lower than in the LDPE/oMMT samples. This could have resulted from the higher affinity between the polyethylene and the kaolinite. SEM (Fig. 4b) and TEM pictures (Fig. 4c,d) show a morphology where the clay particles are well dispersed in the form of aggregates of a few nanometers but with a lower aspect ratio than in the sample of LDPE/PEMA/oMMT. High magnification TEM picture (Fig. 4e) shows an intercalated structure. Regarding aspect ratio (L/T), it is difficult to estimate accurately values giving the dispersion in sizes, platelet shape, and particles orientation, however the average length ($L$) of the aggregates is between 300 and 400 nm and thickness ($T$) between 30 and 100 nm. Individual layers were not observed in this system.

## 3.3. Rheological and mechanical characterization

Melt rheology has been used as a complementary method to analyze the dispersion/exfoliation in polymer–clay nanocomposites. Several authors found that the shear thinning index $n$ gives a semi-quantitative measure of the degree of exfoliation [25].

In this study the complex viscosity and the storage modulus (Fig. 5) were measured at 190 °C in the low angular frequency region by means of a rotational rheometer. It was observed that at low frequencies, none of the samples, including LDPE, displayed a Newtonian plateau. Complex viscosity was found to be dependent on the screw profile, the clay nature or the presence of compatibilizer. The greatest differences between the curves were observed at low angular frequencies. LDPE/PEMA/oMMT exhibited highest complex viscosity and storage modulus which can be correlated to the higher degree of intercalation–exfoliation and to the higher aspect ratio (as observed by TEM). Storage modulus at 0.1 rad/s are 564, 616, 1380, 661 and 460 Pa for LDPE, LDPE/oMMT conf A, LDPE/PEMA/oMMT, LDPE/K and LDPE/oMMT conf B, respectively. These

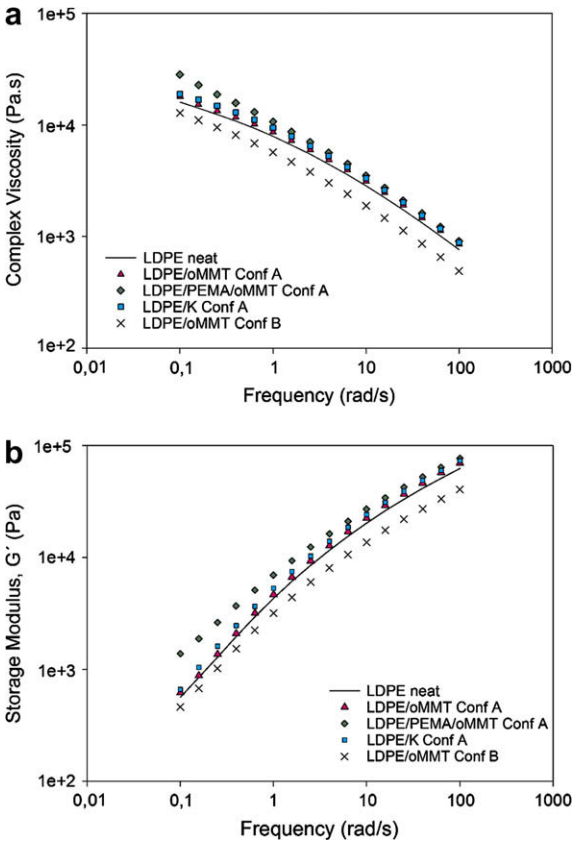


**Fig. 5.** Rheology: (a) complex viscosity; (b) storage modulus.

results may suggest an interaction between the compatibilizer and the clay. Lower complex viscosity and storage modulus were obtained for the microcomposite LDPE/oMMT extruded with screw configuration B, the sample with lowest observed dispersion.

The shear thinning exponents $n$ for the nanocomposites extruded with configuration A were calculated according to the power law expression ($\eta = A\omega^n$) in the low frequency region (between 0.1 and 1 rad/s) and are summarized in Table 2. The addition of clay alone (oMMT or K) to the polyethylene does not affect the shear thinning behaviour, but the addition of 10% of PEMA to the sample LDPE/oMMT increments the shear thinning exponent significantly from 0.31 to 0.41. This could indicate that the nanocomposite with compatibilizer presents a higher degree of clay dispersion. Previous authors have correlated the shear thinning index with the exfoliation level [26].

**Table 2**
Shear thinning exponent ($n$), elastic modulus ($E$), melt strength and breaking speed for nanocomposites prepared with configuration A.

| Sample | $n$ | $E$ (MPa) | Melt strength (cN) | Breaking speed (m/min) |
|---|---|---|---|---|
| LDPE | 0.30 | 109.37 (±4.10) | 21.82 | 16.72 |
| LDPE/oMMT | 0.31 | 114.31 (±6.01) | 16.86 | 11.78[a] |
| LDPE/PEMA/oMMT | 0.41 | 161.52 (±2.11) | 20.19 | 5.15[a] |
| LDPE/K | 0.30 | 170.27 (±10.84) | 27.07 | 13.12 |

[a] Samples with swelling and bubbles.

Elastic modulus of clay nanocomposites depends on the type of clay and the level of exfoliation. No significant improvement was achieved in LDPE/oMMT, probably due to the products originated from the degradation of the modifier substances used in the modification of the montmorillonite that are dispersed in the polymeric matrix. An increase of 48% in the modulus of compatibilized nanocomposite LDPE/PEMA/oMMT was found, which is associated with the higher degree of exfoliation, higher interaction and higher aspect ratio compared to the non-compatibilized LDPE/oMMT sample. Elastic modulus of the nanocomposite LDPE/K increased by 55% with respect to the neat polyethylene as a result of the good dispersion shown in this sample and the use of a clay which was not degraded during the melt mixing.

The presence of free surfactant molecules or degraded compounds dispersed in the polyethylene matrix was found to have a negative effect on the melt strength of the final nanocomposites. Montmorillonite samples show a reduction in the values of melt strength and breaking speed (reduction in the extensibility of the material). This can be attributed to the swelling effect and the presence of bubbles formed as a consequence of the degradation of the modifiers (see Fig. 6). However, nanocomposites formed with kaolinitic clay showed an increase in the melt strength and a small decrease in the melt breaking speed, with respect to neat LDPE. As shown in Fig. 6, the fibre of LDPE/K has a smooth surface without bubbles. This suggests that the nanocomposite with kaolinite may lead to better stability in film extrusion processes, blowing moulding or thermoforming.

### 3.4. In-process ultrasound measurements

Ultrasonic transit time, signal loss (as an indication of attenuation) calculated from the first and the second peaks of the transmitted wave, and the height of the first peak of the wave were measured for each sample.

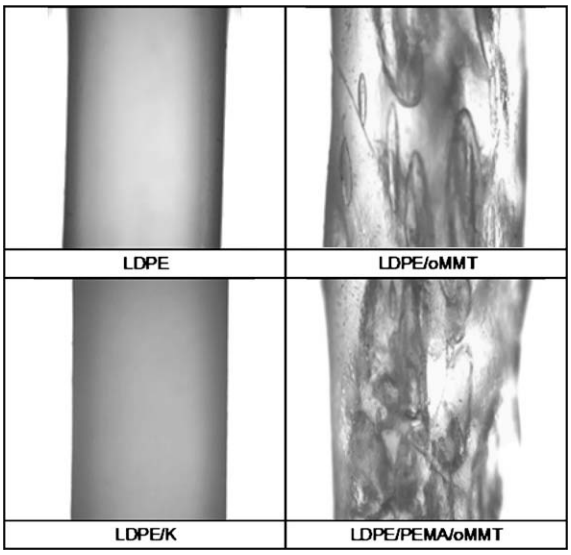


**Fig. 6.** Optical micrographs of fibers obtained in the capillary rheometer during the melt strength tests.

Ultrasonic transit time is indicative of the velocity of propagation of the ultrasonic wave across the measurement medium. This is a function of melt density, bulk modulus, pressure and temperature. The addition of clay caused a general increase in transit time with respect to the neat polymer, up to 57.30 μs in the sample LDPE/oMMT processed with screw configuration A.

Fig. 7a shows the transit time for LDPE/K and LDPE/oMMT composites prepared with screw configuration A, where it can be seen that the time is lower for the sample with kaolinite. This may be correlated with a smaller size of kaolinite aggregates compared to montmorillonite. The same tendency was previously seen in HDPE/carbon black composites [18]. However, there is no direct correlation between the clay dispersion observed by microscopy and the transit time comparing the effect of screw configuration. In this case, transit time can be very sensitive to changes in parameters such as melt density or melt temperature caused by the mixing with the two different screw configurations.

The effect of compatibilizer on transit time for unfilled LDPE was negligible. However, the addition of oMMT to the reference sample LDPE/PEMA increased also the transit time as a consequence of a decrease in the velocity of propagation of the wave. Fig. 7b shows a reduction in transit time in the compatibilized nanocomposite compared to the uncompatibilized one, which could be attributed also to the reduction in oMMT size with the addition of compatibilizer.

Signal loss (or attenuation) increased with the addition of clay. Signal loss appeared to show a clear relationship with the measured dispersion levels observed in the optical, SEM and TEM micrographs discussed previously, with lower signal loss values corresponding to improved dispersion levels. For example, signal loss in LDPE/oMMT was 42.2% using screw configuration 'A'. However, attenuation increased to 45.33% using screw configuration 'B' for which poorer dispersion was observed (higher density of microaggregation at the micrometric scale was observed by MO with configuration B). The lowest signal loss was achieved for LDPE/K (41.28%), in which better clay dispersion was observed (Fig. 7c).

Addition of compatibilizer to montmorillonite filled LDPE nanocomposites caused a significant reduction in attenuation levels, from 53.98% to 47.49% in the nanocomposite with 10% of PEMA and processed with configuration 'A' (Fig. 7d). Subtracting the attenuation values of unfilled LDPE/PEMA from those for LDPE/PEMA/oMMT gives the attenuation levels attributed directly to the clay; in this case, measured attenuation dropped from 18% to 7% due to the better dispersion levels obtained with 10% of compatibilizer. In this way, measurement of ultrasonic attenuation may provide a viable method of monitoring dispersion levels in nanocomposite materials.

Peak height of the first peak of the ultrasonic waveform is another measure of the amount of energy transmitted across the melt and, therefore, potentially another useful source of material information. Peak height was reduced significantly with addition of clay, from 3.39 mV to a minimum of 0.72 mV for LDPE/oMMT extruded with configuration B. Peak height generally exhibited an inverse trend to

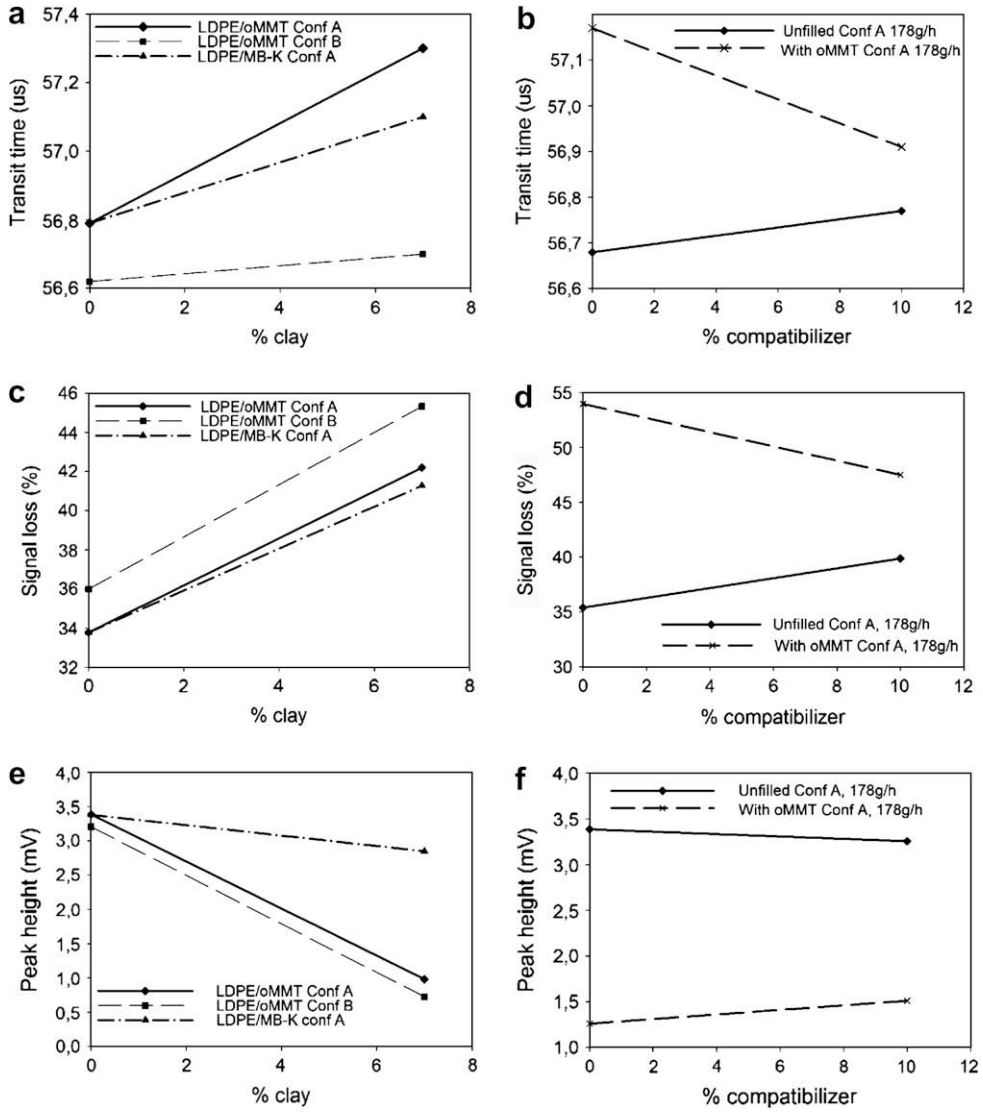


**Fig. 7.** Effect of clay nature and screw configuration on (a) transit time; (c) signal loss; (e) peak height. Effect of compatibilizer on (b) transit time; (d) signal loss; (f) peak height.

attenuation (signal loss), i.e. peak height decreased with addition of clay but increased with improved dispersion.

Peak height values reflected differences between the clay types, as shown in Fig. 7e. Kaolinite nanocomposites showed less of a decrease in peak height with respect to unfilled LDPE. This is likely to be due to the size of kaolinite aggregates being smaller than those in montmorillonite nanocomposites; lower size was observed by microscopy.

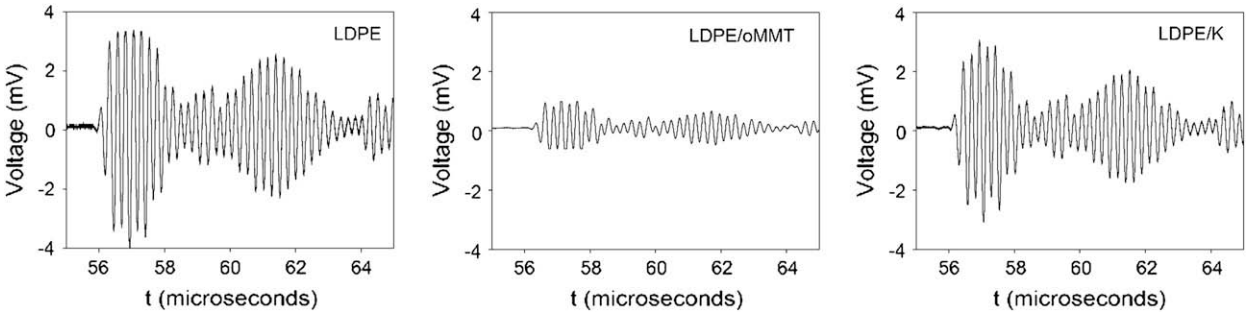


**Fig. 8.** Examples of ultrasound waves transmitted in LDPE and LDPE/clay nanocomposites processed with screw configuration 'A' at 309 g/h.

This parameter showed a slight increment in nanocomposites processed with screw configuration 'A' respect to screw configuration 'B'. The addition of a small content of compatibilizer to the system LDPE/oMMT also reflected in a slight increment of the peak height respect to the non-compatibilized montmorillonite nanocomposites (Fig. 7f). All these results may suggest that peak amplitude is less dependent upon dispersion levels and more dependent upon particle size or size distribution.

Fig. 8 represents three ultrasound waves measured for unfilled LDPE and LDPE nanocomposites with both clays: it is clearly visible that the nanocomposite with montmorillonite resulted in significantly lower energy (i.e. smaller peak amplitude) being transmitted across the melt polymer compared to the unfilled LDPE and to the kaolinite nanocomposite.

## 4. Conclusions

The experimental studies described here were conducted to investigate the effects of screw configuration and clay nature (montmorillonite and kaolinite) on the dispersion, and to assess the potential of in-line ultrasound measurements to monitor dispersion levels.

The screw configuration A, formed by a combination of distributive and dispersive mixing zones, caused better clay dispersion than screw configuration B with a lower degree of mixing and lower residence time.

Modified montmorillonite could not be completely dispersed in polyethylene as the high temperatures used for extrusion caused degradation of the modifiers and the collapse of clay layers. However, the addition of a small percentage of maleated polyethylene (PEMA) facilitated the dispersion of oMMT.

Kaolinite showed a higher affinity than montmorillonite to be dispersed in polyethylene. Kaolinite nanocomposite showed a higher increment in the elastic modulus and melt strength compared to the samples with organomodified montmorillonite.

In-process ultrasonic measurements across melt flow in the extruder die were shown to provide a viable indication of dispersion levels during extrusion process, although the relationships between measured signals and morphology are complex and warrant further investigation. Transit time and attenuation (or signal loss), appeared to provide the most sensitive indication of dispersion levels, being lowest for the most highly dispersed nanocomposites. The peak height of the received ultrasonic signal showed the clearest differences between clay types, possibly due to particle size and distribution.

## Acknowledgements

This work has been financially supported by the project MEC MAT2006-10261-C03. The authors would like to acknowledge to NanoBioMatters, S.L. for supplying the clays and the IRC in Polymer Engineering (University of Bradford, UK) for all the equipments used here. The authors would like to thank Emma L. Burton, Mike Woodhead, Raquel Oliver, Pepe Ortega and to SCIC of the University Jaume I for the experimental support. Finally, M.P. Villanueva would like to thank Generalitat Valenciana for the FPI research grant awarded, the Universitat Jaume I and the Fundació Caixa Castelló-Bancaixa for the international travel research grant.

## References

[1] M. Alexandre, P. Dubois, Polymer-layered silicate nanocomposites: preparation, properties and uses of a new class of materials, Materials Science and Engineering R: Reports 28 (2000) 1.
[2] S.S. Ray, M. Okamoto, Polymer/layered silicate nanocomposites: a review from preparation to processing, Progress in Polymer Science 28 (2003) 1539.
[3] E.P. Giannelis, Polymer-layered silicate nanocomposites: synthesis, properties and applications, Applied Organometallic Chemistry 12 (1998) 675.
[4] A. Durmus, M. Woo, A. Kasgoz, C.W. Macosko, M. Tsapatsis, Intercalated linear low density polyethylene (LLDPE)/clay nanocomposites prepared with oxidized polyethylene as a new type compatibilizer: structural, mechanical and barrier properties, European Polymer Journal 43 (2007) 3737.
[5] T.G. Gopakumar, J.A. Lee, M. Kontopoulou, J.S. Parent, Influence of clay exfoliation on the physical properties of montmorillonite/polyethylene composites, Polymer 43 (2002) 5483.
[6] S. Hotta, D.R. Paul, Nanocomposites formed from linear low density polyethylene and organoclays, Polymer 45 (2004) 7639.
[7] H.R. Dennis, D.L. Hunter, D. Chang, S. Kim, J.L. White, J.W. Cho, D.R. Paul, Effect of melt processing conditions on the extent of exfoliation in organoclay-based nanocomposites, Polymer 42 (2001) 9513.
[8] M. Mehrabzadeh, M.R. Kamal, Melt processing of PA-66/clay, HDPE/clay and HDPE/PA-66/clay nanocomposites, Polymer Engineering and Science 44 (2004) 1152.
[9] F. Chavarria, R.K. Shah, D.L. Hunter, D.R. Paul, Effect of melt processing conditions on the morphology and properties of nylon 6 nanocomposites, Polymer Engineering and Science 47 (2007) 1847.
[10] W. Lertwimolnun, B. Vergnes, Effect of processing conditions on the formation of polypropylene/organoclay nanocomposites in a twin screw extruder, Polymer Engineering and Science 46 (2006) 314.
[11] W. Lertwilmolnun, B. Vergnes, Influence of compatibilizer and processing conditions on the dispersion of nanoclay in a polypropylene matrix, Polymer 46 (2005) 3462.
[12] A.L. Kelly, M. Woodhead, P.D. Coates, D. Barnwell, K. Martin, In-process rheometry studies of LDPE compounds – part II: magnesium hydroxide filled, International Polymer Processing 15 (2000) 361.
[13] S.E. Barnes, E.C. Brown, M.G. Sibley, H.G.M. Edwards, I.J. Scowen, P.D. Coates, Vibrational spectroscopic and ultrasound analysis for in-process characterization of high-density polyethylene/polypropylene blends during melt extrusion, Applied Spectroscopy 59 (2005) 611.
[14] E.C. Brown, P. Olley, P.D. Coates, In-line melt temperature measurement during real time ultrasound monitoring of single screw extrusion, Plastics Rubber and Composites 29 (1) (2000) 3.
[15] L. Erwin, J. Dohner, Measurement of mixing in polymer melts by focused ultrasound, Polymer Engineering and Science 24 (1984) 1277.
[16] C. Verdier, M. Piau, Analysis of the morphology of polymer blends using ultrasound, Journal of Physics D: Applied Physics 29 (1996) 1454.
[17] T.H. Nayfeh, N.H. Abu-Zahra, W.M. Fedak, A.A. Salem, Ultrasound measurement of two-filler concentrations in polypropylene compounds. Part 1: static calibration, International Journal of Advanced Manufacturing Technology 20 (2002) 313.
[18] G.D. Smith, E.C. Brown, D. Barnwell, K. Martin, P.D. Coates, Use of ultrasound to determine variation of carbon dispersion in carbon black filled HDPE melts, Plastics Rubber and Composites 32 (2003) 167.
[19] M. Kato, H. Okamoto, N. Hasegawa, A. Tsukigase, A. Usuki, Preparation and properties of polyethylene-clay hybrids, Polymer Engineering and Science 43 (2003) 1312.
[20] R.K. Shah, D.R. Paul, Organoclay degradation in melt processed polyethylene nanocomposites, Polymer 47 (2006) 4075.
[21] M.D. Sanchez-Garcia, E. Gimenez, J.M. Lagaron, Morphology and barrier properties of nanobiocomposites of poly(3-hydroxybutyrate) and layered silicates, Journal of Applied Polymer Science 108 (2008) 2787.
[22] L. Cabedo, J.L. Feijoo, M.P. Villanueva, J.M. Lagaron, E. Gimenez, Optimization of biodegradable nanocomposites based on aPLA/PCL blends for food packaging applications, Macromolecular Symposia 233 (2006) 191.

[23] L. Cabeda, E. Gimenez, J.M. Lagaron, R. Gavara, J.J. Saura, Development of EVOH–kaolinite nanocomposites, Polymer 45 (2004) 5233.
[24] T. Itagaki, A. Matsumura, M. Kato, A. Usuki, K. Kuroda, Preparation of kaolinite-nylon6 composites by blending nylon6 and a kaolinite–nylon6 intercalation compound, Journal of Materials Science Letters 20 (2001) 1483.
[25] R. Wagener, T.J.G. Reisinger, A rheological method to compare the degree of exfoliation of nanocomposites, Polymer 44 (2003) 7513.
[26] A. Durmus, A. Kasgoz, C.W. Macosko, Linear low density polyethylene (LLDPE)/clay nanocomposites. Part I: structural characterization and quantifying clay dispersion by melt rheology, Polymer 48 (2007) 4492.